Physics and Chemistry of Minerals
https://doi.org/10.1007/s00269-019-01029-x

ORIGINAL PAPER

Theoretical study of lithium diffusion and fractionation in forsterite and its high-pressure phases

Jiajun Jiang[1,2] · Feiwu Zhang[1,3] · Hua Yang[1,2] · Tiancheng Yu[4]

Received: 1 October 2018 / Accepted: 26 February 2019

Abstract

As a geochemical tracer in mantle studies, lithium isotopes play an important role in diffusion and fractionation in major mantle minerals. Olivine and its high-pressure phases, wadsleyite and ringwoodite, are considered to predominate in the upper mantle and transition zone on the earth. We carried out simulations of lithium isotopes' diffusion and fractionation in Mg end member olivine and its high-pressure phases to learn the details of the signatures of lithium isotopes preserved in mantle materials. In this work, the diffusion and fractionation mechanisms between different lattice sites of lithium isotopes in forsterite (Mg_2SiO_4), wadsleyite (β-Mg_2SiO_4) and ringwoodite (γ-Mg_2SiO_4) at the atomic level are studied using empirical atomistic simulation techniques. It is found that Li can pass through the high-pressure phases (wadsleyite and ringwoodite) energetically much easier due to the low migration energy barriers via either substitutional or interstitial mechanism. The activation energy is high for Li diffusion along the interstitial path in the forsterite and decreases drastically with the assist of Mg vacancies. The temperature-dependent fractionation for two Li isotopes between two different lattice sites is calculated at the temperatures from 300 to 2500 K. This behavior generates the lighter Li storage in the near-surface mantle-derived rocks and provides insights into zoning and composition of lithium isotopes in olivine and its high-pressure phases.

Keywords Olivine · Wadsleyite · Ringwoodite · Lithium · Diffusion · Fractionation · Simulation

Introduction

Lithium and its stable isotopes (^{6}Li and ^{7}Li) have received increased attention in recent years as geochemistry tracers of mantle evolution and subduction crust–mantle cycling (e.g., Seitz and Woodland 2000; Woodland et al. 2002; Seitz et al. 2003, 2004; Elliott et al. 2004; Teng et al. 2006; Marschall et al. 2007; Ionov and Seitz 2008; Magna et al. 2015; Trail and Cherniak 2016), which is due to the large variation in Li isotope ratios in natural materials and the structural compatibility of Li in mantle minerals. Because of the large isotopic mass difference, lithium is particularly susceptible to mass-dependent isotope fractionation, even at high temperatures. This process has got increasing recognition by Li partitioning between co-existing phases (Gallagher and Elliott 2009; Strandmann et al. 2011).

Olivine is the major constituent of the upper mantle to depths of 400 km and considerable effort has gone into characterizing the transport properties of this phase under a range of conditions. It was reported that olivine is believed to be a major reservoir of Li in the Earth's upper mantle (Brenan et al. 1998a, b; Seitz and Woodland 2000; Ottolini et al. 2000, 2002) and that Li can substitute for Mg in major mantle minerals such as olivine, pyroxene and garnet (Wood and Blundy 1997; Lodders 2003; Grant and Wood 2010; Cahalan et al. 2014). Dohmen et al. (2010) has found that Li diffusion in olivine occurs via two different mechanisms, as hops among interstitial and substitutional metal sites, which is the same as the properties on Li diffusion in other silicates (Redfern et al. 2005; Richter et al. 2014). The incorporation of Li at interstitial and metal sites in forsterite was also

✉ Feiwu Zhang
zhangfeiwu@vip.gyig.ac.cn

1 State Key Laboratory of Ore Deposit Geochemistry, Institute of Geochemistry, Chinese Academy of Sciences, Guiyang 550081, China

2 University of the Chinese Academy of Sciences, Beijing 100049, China

3 Key Laboratory of Earth and Planetary Physics, Institute of Geology and Geophysics, Chinese Academy of Sciences, Beijing 100029, China

4 School of Mathematics and Physics, Suzhou University of Science and Technology, Suzhou 215009, China

Published online: 04 March 2019

confirmed by quantum mechanical calculations and significant fractionation of Li isotopes between these two types of lattice sites were successfully predicted (Zhang and Wright 2012b), where Li diffusion mechanisms and migration barriers in the forsterite lattice have been calculated at the atomic level. Olivine have two high-pressure phases, wadsleyite and ringwoodite, which predominate in the mantle transition zone (Farber et al. 1994, 2000). The phase transitions of olivine to wadsleyite, and wadsleyite to ringwoodite will happen at ~12GPa (Morishima et al. 1994) and ~15GPa (Suzuki et al. 2000), respectively. It is also reported that Li can exist in majoritic garnet as a non-negligible fraction in the mantle transition zone (Kaminsky et al. 2001; Seitz et al. 2003). However, the diffusion mechanisms of Li and other monovalent ions in the mantle transition zone mineral and its isotope fractionations in the mineral different lattice sites are still not well known. Diffusion is also considered to be a significant reason for partitioning of Li preserved within the minerals and rocks. Partially, inter-mineral partitioning of Li may be relevant for closed system processes where intensive parameters like P and T change during cooling and decompression of the rocks (Coogan et al. 2005; Hanrahan et al. 2009; Yakob et al. 2012) and even lead to significant diffusive isotopic fractionation (Jeffcoate et al. 2007), which also can happen to other major elements, such as Mg (Chopra et al. 2012).

To interpret chemical signatures and diffusion processes in detail over long timescales, in this study, we conducted the computational modeling on the lithium diffusion and fractionation in Mg end member olivine (forsterite) and its high-pressure phases at the conditions of the Earth upper mantle and transition zone. Our theoretical studies will provide an insight into Li diffusion mechanisms at the atomic level, which lead to Li isotopes variation in the mantle rocks. The Li isotope fractionation between different lattice sites was investigated in the present work. The calculated results are able to improve our comprehension on the behavior of chemical exchange, material transport and electrical conductivity in the Earth's upper mantle and transition zone, as well as help us to interpret the observed isotope variations in natural materials.

Methodology

Computer simulation is increasingly being used to illustrate point defect structures and processes in minerals. In this work, defects in forsterite and its high-pressure phase are studied by empirical atomistic simulation techniques based on Born model of solid that employs interatomic potential functions to describe the energy of the system in terms of the atomic coordinates. A large number of defect configurations can be routinely sampled in a much shorter timeframe in a large simulation cell, which would not be possible by employing first-principles approaches. The ability of such models to accurately model defective crystal structures depends critically on the quality and robustness of the potential parameters used. In our calculations, we take fitted potential parameters by Catlow (1977) and Lewis and Catlow (1985) to describe non-bonded interactions between oxygen and the various cations. In addition, we employ three-body terms to describe directionality of the Si–O tetrahedral environment (Sanders et al. 1984). These parameters originally developed for oxides, have been widely and successfully used to model a range of materials with various cation coordination environments (Palin et al. 2003, 2005; Zhang and Wright 2012a). The reliability of the used empirical methods can be also evidenced by their successful employment in the calculations of defective and hydrous forsterite (Béjina et al. 2009; Walker et al. 2006, 2009) and its high-pressure phases, wadsleyite (Wright and Catlow 1996; Walker et al. 2006,) and ringwoodite (Blanchard et al. 2005; Price et al. 1987), where the agreement with experiments and first-principle calculations was excellent. The interatomic potential models calculation had also well predicted the experimental findings in the lithium manganese spinel oxides (Piszora et al. 2000). The full set of impurity oxygen parameters is given in Table 1.

In this study, all calculations are performed with the General Utility Lattice Program (GULP) code (Gale 1997). To limit the effect of defect–defect interactions in the periodic images, we use a 4×2×3 supercell (19.0 Å × 20.4 Å × 18.0 Å) with 672 atoms for forsterite, a 4×2×3 supercell (22.8 Å × 22.9 Å × 24.7 Å) with 1344 atoms for wadsleyite, and a 2×2×2 supercell (16.1 Å × 16.1 Å × 16.1 Å) with 448 atoms for ringwoodite. Geometry optimizations on the defective supercells were performed without imposed symmetry at 0 K.

Isotope fractionation

Within the structures of forsterite and its high-pressure polymorphs, the fractionation of two Li isotopes at substitutional and interstitial sites is denoted by the formula:

$$\alpha_{\text{interstitial-vacancy}} = \frac{\left[^7\text{Li}/^6\text{Li}\right]_{\text{interstitial}}}{\left[^7\text{Li}/^6\text{Li}\right]_{\text{vacancy}}} = \frac{\beta_{\text{interstitial}}}{\beta_{\text{vacancy}}}$$

where $\alpha_{\text{interstitial-vacancy}}$ is the Li isotope fractionation coefficients between interstitial and vacancy substitution mechanisms, and β represents the mass-dependent isotope partition function ratio, which can be calculated by:

$$\beta = Q\left[^7\text{Li}\right]/Q\left[^6\text{Li}\right]$$

where Q represents the mass-dependent isotope partition function. It can be written as:

$$E = -K_B T \ln Q \Rightarrow Q = \exp\left(-\frac{E}{K_B T}\right).$$

Table 1 Set of potentials parameters used in our calculations

Ions	Core	Shell	Core–shell spring constant (eV/Å^2)
Charges			
Li^+	1.00		
Mg^{2+}	2.00		
Si^{4+}	4.00		
O^{2-}	0.8482	− 2.8482	74.90
Buckingham potential			
	A(eV)	ρ(nm)	C (eV•Å^6)
Li^+–O^{2-}	632.0	0.291	0.0
Mg^{2+}–O^{2-}	1430.0	0.295	0.0
Si^{4+}–O^{2-}	1280.0	0.321	10.70
O^{2-}–O^{2-}	22800.0	0.149	27.90
Harmonic three-body potential			
		k (eV/rad^{-2})	θ_0 (degrees)
O^{2-}–Si^{4+}–O^{2-}		2.097	109.47

Atom O was the used core–shell model. The Buckingham potential is written, $\varphi(r_{ij}) = Aexp(-r_{ij}/\rho) - C/r_{ij}^6$, where A, C and ρ are fitted parameters describing the interaction of two species, i and j, separated by a distance r_{ij}, and $\varphi(r_{ij})$ is the contribution to the total energy from this interaction. A cutoff of 10 Å was used for the Buckingham potential. The harmonic three-body term is expressed as 1/2 k (θ – θ_0), θ being the obtuse angle of O–Si–O

Buckingham potential is based on Catlow (1977) and Lewis and Catlow (1985), while the harmonic three-body potential is described by Sanders et al. (1984)

Therefore, the mass-dependent isotope partition function ratio (β) is related to the free energy of the two Li isotopes in the mineral lattice at the certain site:

$$\beta = \exp\left(-\frac{\Delta E}{K_B T}\right) = \exp\left(-\frac{E[^7\mathrm{Li}] - E[^6\mathrm{Li}]}{K_B T}\right)$$

Here ΔE is the difference of Gibbs free energies between two Li isotopes in substitutional or interstitial sites, which is calculated with the same temperature and pressure. K_B is Boltzmann's constant, and T is the temperature in Kelvin. The Gibbs free energies as a function of temperature are calculated through the determination of the vibrational partition function from the phonon density of states through lattice dynamics free energy minimizations.

Defect calculation

Li can be introduced into the lattice as point defect. In the forsterite (4×2×3), wadsleyite (4×2×3), and ringwoodite (2×2×2) supercell, the point defects are built by replacing Mg with Li, or putting Li into an interstitial site. The atomic positions are relaxed again to find an energy minimum representing the Li point defects in the lattice. To find the most energetically favorable Li substitution mechanism, we perform a series of calculations of various defect configurations and compare their formation energies to find the most energetically stable point defect configuration.

The mobility of Li point defects along the diffusion path is determined by moving a Li ion from an initial low energy start point (either vacancy or interstitial site) to an equivalent low energy end point in a few small steps, where the start and end points can be substitutional or interstitial sites. The 2-D optimizations are performed at intervals along the channel within the structure lattice. At each step, the migrating ion under the constraint is not allowed to move in a principal crystallographic direction parallel to the diffusion path, which means that the ion is fixed on the diffusion direction but can be relaxed in the perpendicular plane. In the case of GULP, this procedure is implemented by the Newton–Raphson method with a rational function optimization (RFO) (Banerjee et al. 1985) to locate stationary points, where the inverse Hessian matrix is diagonalised to obtain the eigenvalues and eigenvectors. The RFO optimization algorithm will be able to, in principle, locate various possible transition states starting from a given position. We can plot Li ion displacement energy against the diffusion steps. The difference between the minimum and maximum energy along the pathway defines the barrier of migration in this particular diffusion direction, ignoring the energy cost of creating the point defect.

Results and discussion

Defect species

Li can be incorporated into the pure forsterite and its high-pressure polymorphs lattice as either an interstitial or a substitutional defect at a Mg site, both of which require charge compensation. $Li_i^{\bullet}$ and $Li_{Mg}^{'}$ is represented for the interstitial and substitutional configurations, respectively, in the Kröger–Vink defect notation. Both of them require charge compensation. The possibilities for charge neutrality of Li incorporated in the pure lattice can be described as:

(a) $Li_i^{\bullet} + Li_{Mg}^{'}$, where the interstitial Li is isolated from the substitutional Li, or,
(b) $2Li_i^{\bullet} + V_{Mg}^{''}$, where the two interstitial ions are around the vacancy ($V_{Mg}^{''}$)

Zhang and Wright (2012b) has confirmed that the first incorporation mechanism involved Li substitution at an Mg site, with a Li interstitial in forsterite lattice, which is the assumption in Dohmen et al. (2010) and Grant and Wood (2010) as well.

Forsterite has two crystallographic Mg sites, Mg1 and Mg2. Our calculations suggested that Li substitution is energetically favored at the Mg1 site by ~0.85 eV. There are three Mg sites in the wadsleyite lattice, Li substitution at Mg1 site is energetically favorable than Mg2 site by ~0.5 eV and 0.35 eV for Mg3 site. Only one type of Mg site exists in ringwoodite structure, Li incorporated in ringwoodite as substitutional defect at Mg site is simplex. The detailed energy values for different point defects are listed in Table 2. It should be noted that the absolute value in the table does not have any physical meaning, the formation energy defined by the difference between different configurations describes the defects' stabilities and the energy cost to create the defect.

In this work, we consider the Li incorporation mechanism into the pure minerals, however, in natural olivine and its high-pressure phases, with its various minor and trace elements, the possibilities for charge compensation are much more varied. Previous works indicated that both trivalent cations M^{3+} (e.g., Al^{3+}, Fe^{3+} or REE) (Purton 1997; Zhang and Wright 2010, 2012a; Grant and Wood 2010) and monovalent cation (e.g., H^{+}) (Zhang and Wright 2010; Grant and Wood 2010) could be considered as the compensating ions.

Lithium isotopic fractionation

To confirm the extent of Li fractionation in forsterite and its high-pressure polymorphs, we calculated Li isotope fractionation between interstitial and substitutional mechanisms using the methods described in Sect. 2. Table 3 lists the calculated fractionation factors under the certain conditions of different temperature and pressure. We calculated the temperature from 300K to 2500K for the three minerals, while the pressure selection varies due to the different pressure ranges in which they can stably exist. We chose 0 and 12GPa for forsterite, 12 and 15GPa for wadsleyite and 15 and 20GPa for ringwoodite. The empirical methods calculated Li isotope fractionation factors in forsterite in this study (e.g., 49.5‰ and 0.8‰ at 300 K and 2500 K respectively) which are quite similar to what we had previously obtained using the first-principles method (87.1‰ and 1.1‰) (Zhang and Wright 2012b). Both methods have demonstrated, as expected, that temperature is a key factor for Li isotope fractionation.

This study further confirmed that temperature is the key factor for Li isotope fractionation in all the minerals, while pressure has little effect on the fractionation factors. The temperature and pressure effects are evidenced by the calculated isotope fractionation factor, for instance, dropping by the factor of ~10 from the temperature of 300 K to 1000 K and changing by only 0.1% from the pressure of 0 to 12 GPa at 300 K in the forsterite lattice. It was reported that isotopic effect arises mainly from the difference between the vibration energies of the lithium isotopic species. Therefore, the isotope fractionation is the function of the bond energy in the stable isotope systems (e.g., Wenger and Armbruster 1991; Yamaji et al. 2001). For the lighter Li (^{6}Li), it prefers to form a lower-energy bond compared to ^{7}Li, while low bond energy is related to a higher coordination number site. Thus, Li substituting Mg in octahedral mineral sites (e.g., olivine and pyroxenes) will be isotopically lighter than Li found in fluid, which is believed to be in tetrahedral coordination (Wenger and Armbruster 1991; Yamaji et al. 2001). Our fractionation calculations are able to interpret this knowledge. All the values of calculated isotope fractionation factor α are greater than 1 as shown in Table 2, which suggests that heavier Li isotopes will be preferentially

Table 2 Lattice energies for the defective supercells of forsterite (4×2×3), wadsleyite (4×2×3) and ringwoodite (2×2×2)

Defect species	Lattice energies for the defective and perfect supercells (eV)		
	Forsterite (4×2×3)	Wadsleyite (4×2×3)	Ringwoodite (2×2×2)
V''_{Mg1}	− 20344.30	− 40680.93	− 13533.25
V''_{Mg2}	− 20342.40	− 40679.91	
V''_{Mg3}		− 40680.60	
Li'_{Mg1}	− 20352.60	− 40689.07	− 13540.83
Li'_{Mg2}	− 20351.75	− 40688.57	
Li'_{Mg3}		− 40688.72	
$Li^{\bullet}_{i}$	− 20373.12	− 40708.94	− 13558.36
Perfect supercell	− 20368.02	− 40704.52	− 13556.05

The perfect supercell energies are given as well

The defect species are in the Kröger–Vink defect notation. In different minerals, Mg1 and Mg2 do not represent the same types of Mg site. The numbers of Mg (e.g., Mg1, Mg2, Mg3) just represent the amount of Mg site species in the certain mineral lattice. $Li^{\bullet}_{i}$ is the most stable interstitial site we have found in the forsterite, wadsleyite and ringwoodite lattice

Table 3 The force field modeling combined relevant empirical potential calculated fractionations between isotope Li species incorporated in the (a) forsterite, (b) wadsleyite and (c) ringwoodite structures via the interstitial and vacancy substitution mechanisms

Temperature (K)	Pressure (GPa)	Mass-dependent isotope partition function ratio		Isotope fractionation factor
		$\beta_{interstitial}$	$\beta_{vacancy}$	$\alpha_{inter-vac}$
(a)				
300	0	1.42043	1.35344	1.04950
	12	1.44638	1.38031	1.04787
1000	0	1.27380	1.26754	1.00493
	12	1.27716	1.27059	1.00517
1500	0	1.26559	1.26288	1.00214
	12	1.26722	1.26416	1.00243
2000	12	1.26374	1.26194	1.00142
2500	12	1.26203	1.26095	1.00085
(b)				
300	12	1.48144	1.39894	1.05898
	15	1.48654	1.40570	1.05752
1000	12	1.28152	1.27222	1.00731
	15	1.28206	1.27284	1.00724
1500	12	1.26913	1.26492	1.00333
	15	1.26938	1.26523	1.00328
2000	12	1.26476	1.26239	1.00188
	15	1.26492	1.26259	1.00184
2500	12	1.26271	1.26119	1.00120
	15	1.26283	1.26131	1.00121
(c)				
300	15	1.59206	1.40180	1.13573
	20	1.60074	1.41179	1.13384
1000	15	1.29298	1.27259	1.01603
	20	1.29397	1.27357	1.01602
1500	15	1.27427	1.26510	1.00725
	20	1.27475	1.26554	1.00728
2000	15	1.26766	1.26249	1.00410
	20	1.26795	1.26275	1.00412
2500	15	1.26459	1.26129	1.00261
	20	1.26479	1.26148	1.00262

incorporated into forsterite and its high-pressure polymorphs via the interstitial mechanism, while the lighter one will be enriched at Mg sites. At the same temperature, fractionations($\alpha_{inter-vac}$) between isotope Li species have the relation as: forsterite < wadsleyite < ringwoodite, which predicts the greater Li isotopic fractionation takes place at the high-pressure phases, and much more ^{7}Li will be involved in interstitial sites comparing the high-pressure phases to forsterite.

Li migration

Isotopic and chemical heterogeneities existed in natural mantle minerals, and diffusion is one of the significant reasons for differentiation. Discussing the diffusion in the minerals contributes to the reason of elements' partition and the microcosmic mechanism of ionic diffusion. Generally, ions in minerals are considered to be diffused by either the vacancy mechanism or interstitial mechanism (the migration of ions from one interstitial site to the next). Li^{+} is a monovalent cation with a minor radius, which leads to its high mobility in the mineral lattice. Considering that Li can be incorporated into lattice as both interstitial and substitutional point defects, we have considered migration via Mg vacancies, via interstitial sites, and even via interstitial combined vacancy paths. For each path, we calculated the activation energy for migration which can be used to measure ionic mobility along the corresponding route.

There are some possible paths for Li diffusion in forsterite, wadsleyite and ringwoodite lattice as illustrated in Fig. 1.

Li migration in forsterite

This part of work repeated the previous density functional theory calculations on the lithium defects and diffusivity in forsterite (Zhang and Wright 2012b). But this work was conducted by force field modeling, which is much faster and allow us to simulate much larger systems. For forsterite (Fig. 1a), there are four possible vacancy jumping routes: A, from Mg1 to Mg1; D, from Mg2 to Mg2; between Mg1 and Mg2, hops can be B and C, which are approximately symmetric to each other on the plane [100]. E and F represent the interstitial routes, hopping along the [001] and [010] directions, respectively.

In our calculations, Li diffusion by a pure vacancy mechanism has the lowest migration barrier (0.254 eV) along the [001] direction as hop D, which shows similar trends to the calculations by Walker et al. (2009) for Mg, who found a low activation energy in the [001] direction compared to [100] and [010].

Coming to the interstitial mechanism, we find that hop E acquires 0.369 eV energy for migration between site *a* and *b*, and the path for E is flat, apparently. As Li moves to *b* site, the most stable interstitial site in the forsterite lattice, there are two possible conditions for further migration. First, Li at *b* site can move to the other equivalent stable site *b′* by overcoming a very high activation energy via hop F (3.245 eV). However, if there is a vacancy around on either Mg1 or Mg2 sites, the displaced Mg on Mg1 site will move into it and Li will occupy the new Mg1 vacancy. Then, Li will move to the second interstitial site *b′*. The overall process of Li migration from *b* to *b′* assisted with Mg1 vacancy (hop F_v) and results in a 0.844 eV energy decrease compared to hop F.

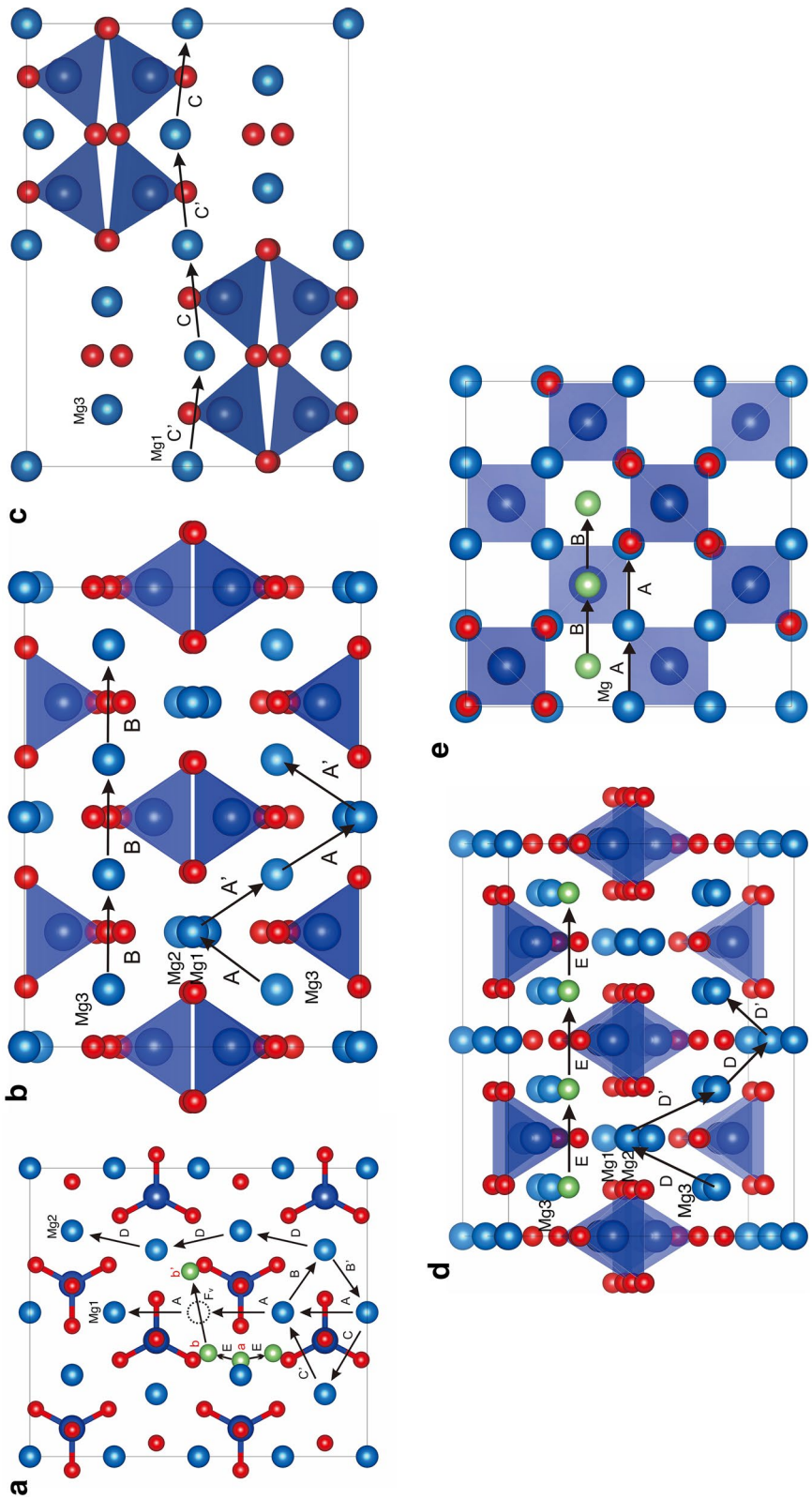

Fig. 1 The calculated possible diffusion paths in forsterite and its high-pressure phases. **a** Possible migration pathways of lithium in forsterite lattice viewed along [100]; **b–d** possible Li diffusion pathways in wadsleyite looking along **b** [010] and **c** [100] directions, and **d** paralleled to [100] direction as well; **e** lithium diffusion in ringwoodite via vacancy and interstitial mechanism along direction [100]

Li migration in wadsleyite

In the lattice of wadsleyite (Fig. 1b–d), parallel to [010], we have two possible paths for Li migration: B involves vacancy hopping from Mg3 to Mg3 sites, and E is an interstitial path also parallel to B. Along the plane [100], C can be the possible path between Mg1 and Mg2, while vacancy hops, A (between Mg1 and Mg3) and D (between Mg2 and Mg3), are of all three principal crystallographic directions.

We find that hop A has the lowest diffusion activation energy (0.110 eV) for Li migration by the vacancy mechanism. The calculations can simply interpret by the lower energy of Li'_{Mg1} and Li'_{Mg3} compared to Li'_{Mg2}, which leads to easier Li diffusion between Mg1 and adjacent Mg3 sites. In other words, Mg2 is associated with high energy reflected by the high diffusion energy of Li along the relevant hops (C of 0.597 eV and D of 1.392 eV).

Besides, hop E acquires 0.533 eV for Li migration representing the diffusion activation energy of Li by the interstitial mechanism. The value decreases rapidly compared to the same diffusion mechanism in forsterite.

Li migration in ringwoodite

Li diffusion in pure ringwoodite lattice can be more simple than the other two (Fig. 1e). There are two possible hops (A and B) among the Mg vacancies and interstitial sites. Due to the lattice isotropy of ringwoodite, possible paths, A and B, both can have three directions for migration: A is related to [101], [110], [011] directions, while Li diffuses along B in the three principal crystallographic directions, [100], [010], [001]. The diffusion activation energies required for Li to migrate in ringwoodite are 0.261 eV and 0.257 eV of path A and B, respectively, Table 4 gives the calculated diffusion activation energy for each Li path, while the energy profiles are detailed in Fig. 2. These values represent the Li ion diffusion barrier ignoring the background energy associated with defective lattice. We noted that Li diffusion activation energies in high-pressure phases among interstitial sites have sharply decreased compared to forsterite (Table 5), which indicated that it becomes easier for Li migration by the interstitial mechanism as the pressure increases.

Consequently, as pressure increases, we get two conclusions: (1) referring to Sect. 3.2., we consider that more ^{7}Li

Table 4 Li diffusion activation energies in the forsterite and its high-pressure polymorphs lattices along various possible paths viewed in Fig. 1

Possible paths	Li migration activation energy (eV)
(a) Activation energies of several Li diffusion paths in the forsterite lattice marked in Fig. 1(a)	
Vacancy diffusion	
A	0.254
B	1.343
C	0.987
D	1.299
Interstitial diffusion	
E	0.369
F	3.245
Vacancy-assisted interstitial diffusion	
Fv	0.844
(b) Activation energies of several Li diffusion paths in the wadsleyite lattice marked in Fig. 1c–e	
Vacancy diffusion	
A	0.110
B	0.201
C	0.597
D	1.392
Interstitial diffusion	
E	0.533
(c) Activation energies of several Li diffusion paths in the wadsleyite lattice marked in Fig. 1b	
Vacancy diffusion	
A	0.261
Interstitial diffusion	
B	0.257

can be incorporated into interstitial sites. (2) Additionally, it becomes easier for Li migration by the interstitial mechanism. Combining these two points, we infer that high-pressure phases have low contents of ^{7}Li, on account of that much more ^{7}Li migrate out of minerals by the interstitial mechanism, while forsterite has the enrichment of ^{7}Li, relatively. Thus, compared with wadsleyite and ringwoodite, forsterite may have a heavier composition of Li isotopes.

In the Li diffusion experiment researches, the whole diffusion processes in forsterite were measured neglecting the independent influences of different steps in the integrated process (Parkinson et al. 2007; Dohmen et al. 2010; Spandler and O'Neill 2010). Moreover, such Li diffusion experiments of wadsleyite and ringwoodite are not found, as yet. Computer simulation researches in this study explain the detailed stages of the overall diffusion mechanism and calculate the activation energies for individual paths, which provide complementary information and understanding of diffusion on the atomistic scale in both forsterite and its high-pressure phases.

The modeling of Li diffusion mechanism in this study suggests that Li diffusion in forsterite via a purely interstitial mechanism is greatly impossible. That is in accordance with Zhang and Wright (2012b) who considered Li diffusion in forsterite by way of the vacancy-assisted interstitial mechanism. As denoted in Parkinson et al. (2007), the slower speed of Li diffusion in olivine was proved compared to other minerals, which may be caused by the difficult and complex diffusion mechanism of lithium in olivine. Like that, Li diffusion rates are some orders of magnitude faster than cations such as Mg and Fe in clinopyroxene and plagioclase (Richter et al. 2003; Coogan et al. 2005). This may due to preferable presence and mobility of interstitial Li in these mineral structures. Comparatively, wadsleyite and ringwoodite have more a straightforward path with lower energy for Li diffusion, and a faster cation diffusion compared to olivine was proved in Farber et al. (1994, 2000). Considering the discussion of ions' diffusion above, we infer that activation energy of cation diffusion may be related to the speed, closely. The inference can also be reflected in Mg diffusion in olivine. A low activation barrier had been found in the [001] direction compared to [100] and [010] (Walker et al. 2009), while the [001] direction has the fastest diffusion for Mg diffusion in olivine (e.g., Béjina et al. 2009). However, the thorough relation between diffusion speed and activation energy is complex, which needs more exploration on relevant quantification researches.

As we found, where temperatures are higher, both Li isotopes will be able to migrate through the forsterite via vacancy-assisted interstitial mechanism. And in the high-pressure phases of forsterite, Li can migrate through the lattice via both vacancy and interstitial mechanism with lower energy probably resulting in low content of it. Diffusion rates of mechanisms related to Mg vacancy (vacancy assisted interstitial or pure vacancy mechanism) will be influenced by the concentration of Li point defects and the rate of Mg–Li exchange in calculated minerals, which is complex and difficult to simulate. At the lower temperature, the heavy isotope will be settled in interstitial sites, while the light one is more mobile to migrate out of minerals into magma, which would lead to the lighter Li storage in the near-surface mantle-derived rocks. Certainly, as we mentioned above, natural minerals have kinds of impurities such as trivalent cations and the presence of them could affect the behaviors of Li isotopes and accelerate the absorption of Li to compensate charges. This idea has been proved in several upper mantle minerals, such as olivine (Zhang and Wright 2010, 2012a) and orthopyroxene (Van Westrenen et al. 2000). However, considering the low concentration of such ions in the natural minerals, their influences on Li diffusion rates at the atomic level could be ignored.

Table 5 Activation energies of Li diffusion in the forsterite and its high-pressure phases lattices by vacancy and interstitial mechanism, even the vacancy-assisted interstitial mechanism

Mineral	Activation energies of Li diffusion through different mechanisms (eV)		
	Vacancy mechanism	Interstitial mechanism	Vacancy-assisted interstitial mechanism
Forsterite	0.254	3.245	0.369
Wadsleyite	0.110	0.533	
Ringwoodite	0.261	0.257	

Implications

Li can diffuse out of forsterite and its high-pressure polymorphs via substitutional mechanism with Mg vacancies around in the lattice. This migration progress is mainly controlled by the concentration of Mg vacancies and Li–Mg exchange rate. It is complex to measure impurities migration among Mg sites. For example, with the circumstance of low concentration of Mg vacancies, Li migration via substitutional mechanism may combine with the movements of Mg to offer a channel for diffusion along the energetically preferred direction. Thus, the part of energy for the Mg movements will contribute to the total energy cost for Li diffusion by this mechanism.

By comparing the diffusion activation energies along all possible paths in our calculations and reported Li diffusion rates, we conclude an intimate connection between energies and rates of diffusion, which involves more thermodynamic and kinetic progress. Fractionation calculations of lithium provide a view on the geochemical characteristics of lithium.

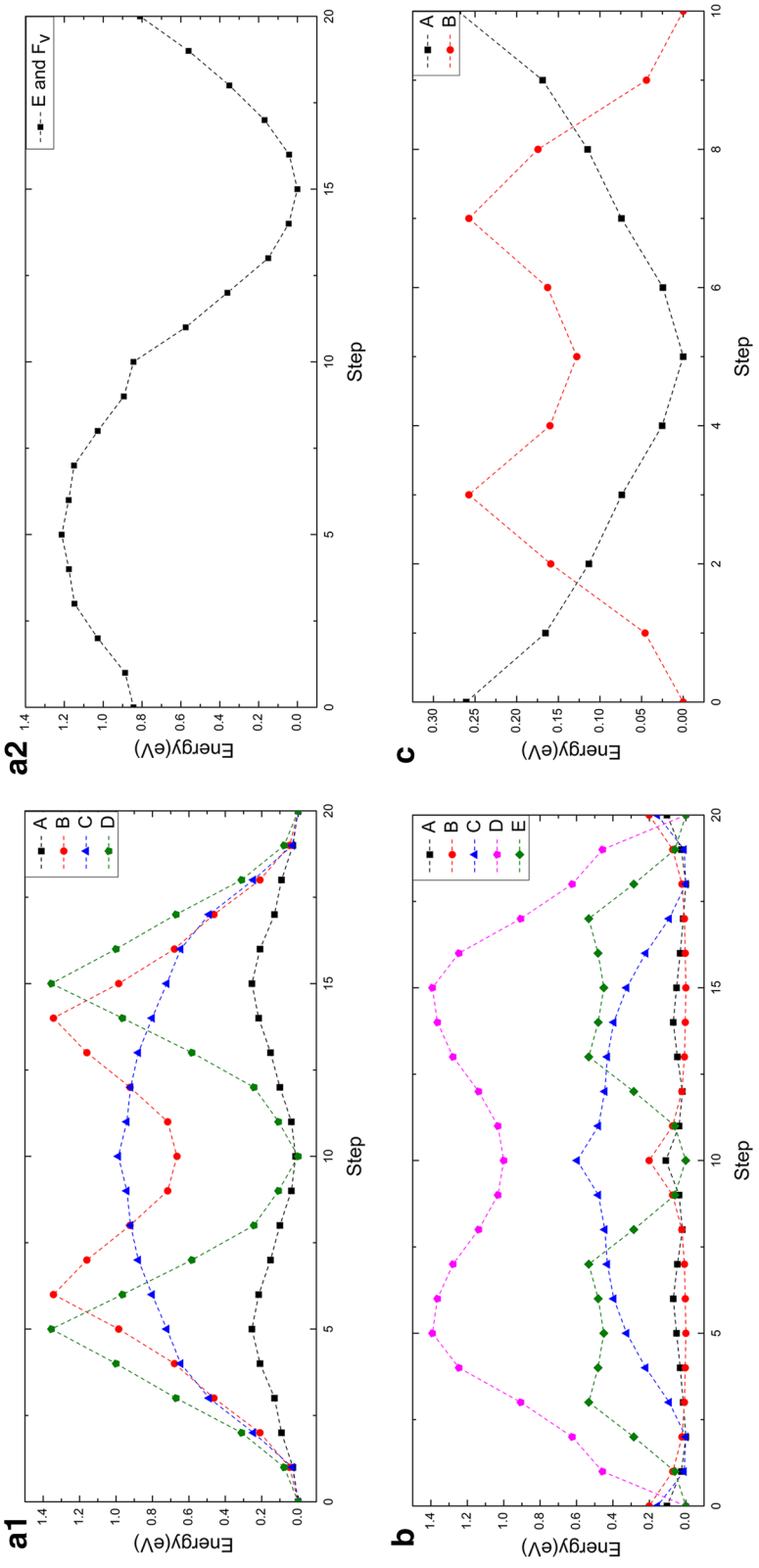

Fig. 2 Energy profiles for lithium diffusion by several possible paths in the forsterite, wadsleyite and ringwoodite. **a** (1) Energy profiles for Li diffusion in forsterite by hops A, B, C and D. (2) and the vacancy-assisted interstitial hops E(from step 0 to step 10) and F_v (from step 10 to step 20) (bottom). **b** Energy profiles for Li diffusion in wadsleyite along hops A, B, C, D and E. **c** Energy profiles for Li diffusion in ringwoodite along hops A and B

We considered that the differential partition of Li isotopes between interstitial and substitutional sites might be the prime mechanism for Li isotopic fractionation in the major mantle-derived Li reservoirs.

The previous studies of lithium diffusion in experiments ((Parkinson et al. 2007; Dohmen et al. 2010; Spandler and O'Neill 2010) have given an integrated process of Li diffusion, which are limited in the detailed Li behaviors in the mineral lattices. Our simulations provide evidence on the different stages of Li diffusion in the minerals at the atomic level and give the activation energies of each possible path. This set of methods for Li diffusion calculations could be applied to other mantle minerals. Comprehensive researches of Li diffusion in major mantle minerals may provide clues to chemical heterogeneity preserved in the upper mantle and transition zone.

Acknowledgements We thank Prof. Julian Gale for providing the latest version of GULP package. This work was supported by the Hundred Talent Program of the Chinese Academy of Sciences (CAS), China National Thousand (Young) Talents plan, National Natural Science Foundation of China (41773057), with computational resources from Computer Simulation Lab, IGGCAS and National Supercomputer Center in Shenzhen, China.

References

Banerjee A, Adams N, Simons J, Shepard R (1985) Search for stationary points on surfaces. J Phys Chem 89:52–57

Béjina F, Blanchard M, Wright K, Price GD (2009) A computer simulation study of the effect of pressure on Mg diffusion in forsterite. Physics of the Earth Planetary Interiors 172(1–2):13–19

Blanchard M, Wright K, Gale JD (2005) A computer simulation study of OH defects in Mg_2SiO_4 and Mg_2GeO_4 spinels. Phys Chem Mineral

Brenan JM, Neroda E, Lundstrom CC, Shaw HF, Ryerson FJ, Phinney DL (1998a) Behaviour of boron, beryllium, and lithium during melting and crystallization: constraints from mineral-melt partitioning experiments. Geochimica Et Cosmochimica Acta 62(12):2129–2141

Brenan JM, Ryerson FJ, Shaw HF (1998b) The role of aqueous fluids in the slab-to-mantle transfer of boron, beryllium, and lithium during subduction: experiments and models. Geochimica Et Cosmochimica Acta 62(19–20):3337–3347

Cahalan RC, Carlson ED, William D (2014) Rates of Li diffusion in garnet: Coupled transport of Li and Y + REEs. Am Miner 99(8–9):1676–1682

Catlow CRA (1977) Oxygen incorporation in the alkaline earth fluorides. J Phys Chem Solids 38(10):1131–1136

Chopra R, Richter FM, Watson EB, Scullard CR (2012) Magnesium isotope fractionation by chemical diffusion in natural settings and in laboratory analogues. Geochim Et Cosmochim Acta 88(88):1–18

Coogan LA, Kasemann SA, Chakraborty S (2005) Rates of hydrothermal cooling of new oceanic upper crust derived from lithium-geospeedometry. Earth Planet Sci Lett 240(2):415–424

Dohmen R, Kasemann SA, Coogan L, Chakraborty S (2010) Diffusion of Li in olivine. Part I: Experimental observations and a multi species diffusion model. Geochim Cosmochim Acta 74(1):274–292

Elliott T, Jeffcoate A, Bouman C (2004) The terrestrial Li isotope cycle: light-weight constraints on mantle convection. Earth Planet Sci Lett 220(3–4):231–245

Farber DL, Williams Q, Ryerson FJ (1994) Diffusion in Mg2SiO4 polymorphs and chemical heterogeneity in the mantle transition zone. Nature 371(6499):693–695

Farber DL, Williams Q, Ryerson FJ (2000) Divalent cation diffusion in Mg_2SiO_4 spinel (ringwoodite), β phase (wadsleyite), and olivine: Implications for the electrical conductivity of the mantle. J Geophys Res Atmospheres 105(B1):513–529

Gale JD (1997) GULP: a computer program for the symmetry-adapted simulation of solids. J Chem Soc Faraday Trans 93(4):629–637

Gallagher K, Elliott T (2009) Fractionation of lithium isotopes in magmatic systems as a natural consequence of cooling. Earth Planet Sci Lett 278(3–4):286–296

Grant KJ, Wood BJ (2010) Experimental study of the incorporation of Li, Sc, Al and other trace elements into olivine. Geochim Et Cosmochim Acta 74(8):2412–2428

Hanrahan M, Brey G, Woodland A, Altherr R, Seitz HM (2009) Towards a Li barometer for bimineralic eclogites: experiments in CMAS. Contrib Miner Petrol 158(2):169–183

Ionov DA, Seitz HM (2008) Lithium abundances and isotopic compositions in mantle xenoliths from subduction and intra-plate settings: Mantle sources vs. eruption histories. Earth Planet Sci Lett 266(3–4):316–331

Jeffcoate AB, Elliott T, Kasemann SA, Ionov D, Cooper K, Brooker R (2007) Li isotope fractionation in peridotites and mafic melts. Geochimica Et Cosmochimica Acta 71(1):202–218

Kaminsky F, Zakharchenko O, Davies R, Griffin W, Khachatryan-Blinova G, Shiryaev A (2001) Superdeep diamonds from the Juina area, Mato Grosso State, Brazil. Contributions to Mineralogy and Petrology, 140(6), 734–753

Lewis GV, Catlow CRA (1985) Potential models for ionic oxides. J Phys C Solid State Phys 18(6):1149–1161

Lodders K (2003) Solar system abundances and condensation temperatures of the elements. Astrophys J 591(2):1220–1247

Magna T, Day J, Mezger K, Fehr MA, Dohmen R, Aoudjehane HC, Agee CB (2015) Lithium isotope constraints on crust?ï£ªmantle interactions and surface processes on Mars. Geochim Et Cosmochim Acta 162:46–65

Marschall HR, Seitz HM, Elliott T, Niu Y (2007) The lithium isotopic composition of orogenic eclogites and deep subducted slabs. Earth Planet Sci Lett 262(3–4):563–580

Morishima H, Kato T, Suto M, Ohtani E, Urakawa S, Utsumi W, Shimomura O, Kikegawa T (1994) The phase boundary between agr- and beta-Mg_2SiO_4 determined by in situ X-ray observation. Science 265(5176):1202–1203

Ottolini L, Bigi F, and Simona (2000) An investigation of matrix effects in the analysis of fluorine in humite-group minerals by EMPA, SIMS, and SREF. Am Miner 85(1):89–102

Ottolini L, Hawthorne F, Stirling FC, John (2002) SIMS matrix effects in the analysis of light elements in silicate minerals: Comparison with SREF and EMPA data. Am Miner 87(10):1477–1485

Palin EJ, Guiton BS, Craig MS, Welch MD, Dove MT, Redfern SAT (2003) Computer simulation of Al-Mg ordering in glaucophane and a comparison with infrared spectroscopy. Eur J Miner 15(5):893–901

Palin EJ, Dove MT, Welch MD, Redfern SAT (2005) Computational investigation of Al/Si and Al/Mg ordering in aluminous tremolite amphiboles. Mineral Mag 69(1):1–20

Parkinson IJ, Hammond SJ, James RH, Rogers NW (2007) High-temperature lithium isotope fractionation: Insights from lithium isotope diffusion in magmatic systems. Earth Planet Sci Lett 257(3–4):609–621

Piszora P, Catlow CRA, Woodley SM, Wolska E (2000) Relationship of crystal structure to interionic interactions in the lithium–manganese spinel oxides. Comput Chem 24(5):609–613

Price GD, Parker SC, Leslie M (1987) The lattice dynamics and thermodynamics of the Mg_2SiO_4 polymorphs. Phys Chem Miner 15(2):181–190

Purton JA, Allan NL, Blundy JD (1997) Calculated solution energies of heterovalent cations in forsterite and diopside: Implications for trace element partitioning. Geochimica Et Cosmochimica Acta 61(18):3927–3936

Redfern SAT, Wells SA, Sartbaeva A (2005) Ionic diffusion in quartz studied by transport measurements, SIMS and atomistic simulations. J Phys Condensed Matter 17(7):1099–1112

Richter FM, Davis AM, Depaolo DJ, Watson EB (2003) Isotope fractionation by chemical diffusion between molten basalt and rhyolite. Geochimica Et Cosmochimica Acta 67(20):3905–3923

Richter F, Watson B, Chaussidon M, Mendybaev R, Dan R (2014) Lithium isotope fractionation by diffusion in minerals. Part 1: Pyroxenes. Geochimica Et Cosmochimica Acta 126(2):352–370

Sanders MJ, Leslie M, Catlow CRA (1984) Interatomic potentials for SiO_2. Jchemsocchemcommun 19(19):1271–1273

Seitz HM, Woodland AB (2000) The distribution of lithium in peridotitic and pyroxenitic mantle lithologies - an indicator of magmatic and metasomatic processes. Chem Geol 166(1–2):47–64

Seitz HM, Brey GP, Stachel T, Harris JW (2003) Li abundances in inclusions in diamonds from the upper and lower mantle. Chem Geol 201(3–4):307–318

Seitz HM, Brey GP, Lahaye Y, Durali S, Weyer S (2004) Lithium isotopic signatures of peridotite xenoliths and isotopic fractionation at high temperature between olivine and pyroxenes. Chem Geol 212(1–2):163–177

Spandler C, O'Neill HSC (2010) Diffusion and partition coefficients of minor and trace elements in San Carlos olivine at 1,300 °C with some geochemical implications. Contrib Miner Petrol 159(6):791–818

Strandmann PAEPV, Elliott T, Marschall HR, Coath C, Lai YJ, Jeffcoate AB, Ionov DA (2011) Variations of Li and Mg isotope ratios in bulk chondrites and mantle xenoliths. Geochimica Et Cosmochimica Acta 75(18):5247–5268

Suzuki A, Ohtani E, Morishima H, Kubo T, Kanbe Y, Kondo T, Okada T, Terasaki H, Kato T, Kikegawa T (2000) In situ determination of the phase boundary between Wadsleyite and Ringwoodite in Mg_2SiO_4. Geophys Res Lett 27(6):803–806

Teng FZ, Rudnick WF, Walker RL, Sirbescu RJ, Mona-Liza C (2006) Lithium isotopic systematics of granites and pegmatites from the Black Hills, South Dakota. Am Miner 91(10):1488–1498

Trail D, Cherniak DJ (2016) Li zoning in zircon as a potential geospeedometer and peak temperature indicator. Contrib Miner Petrol 171(3):1–15

Walker AM, Demouchy S, Wright K (2006) Computer modelling of the energies and vibrational properties of hydroxyl groups in α- and β-Mg_2SiO_4. Eur J Mineral 18(5):529–543

Walker AM, Woodley SM, Slater B, Wright K (2009) A computational study of magnesium point defects and diffusion in forsterite. Phys Earth Planet Inter 172(1–2):20–27

Wenger M, Armbruster T (1991) Crystal chemistry of lithium: oxygen coordination and bonding. Eur J Mineral 3(2):387–399

Westrenen WV, Blundy JD, Wood BJ (2000) Effect of Fe^{2+} on garnet - melt trace element partitioning: experiments in FCMAS and quantification of crystal-chemical controls in natural systems. Lithos 53(3–4):189–201

Wood BJ, Blundy JD (1997) The effect of cation charge on crystal-melt partitioning of trace elements. Earth Planet Sci Lett 188(1–2):59–71

Woodland AB, Seitz HM, Altherr R, Marschall H, Olker B, Ludwig T (2002) Li abundances in eclogite minerals: a clue to a crustal or mantle origin? Contrib Miner Petrol 144(1):128–130

Wright K, Catlow CRA (1996) Calculations on the energetics of water dissolution in wadsleyite. Phys Chem Miner 23(1):38–41

Yakob JL, Feineman MD, Deane JA, Eggler DH, Penniston-Dorland SC (2012) Lithium partitioning between olivine and diopside at upper mantle conditions: an experimental study. Earth Planet Sci Lett 329(5):11–21

Yamaji K, Makita Y, Watanabe H, Sonoda A, Kanoh H, Hirotsu T, A., and Ooi K (2001) Theoretical estimation of lithium isotopic reduced partition function ratio for lithium ions in aqueous solution. J Phys Chem A 105(3):602–613

Zhang F, Wright K (2010) Coupled (H^+,M^{3+}) substitutions in forsterite. Geochimica Et Cosmochimica Acta 74(74):5958–5965

Zhang F, Wright K (2012a) Coupled (Li^+, Al^{3+}) substitutions in hydrous forsterite. Am Miner 97(2–3):425–429

Zhang F, Wright K (2012b) Lithium defects and diffusivity in forsterite. Geochimica Et Cosmochimica Acta 91(5):32–39